Journal of Computer Assisted Tomography
11(1):7–16, January/February

Contrast in Rapid MR Imaging: T1- and T2-Weighted Imaging

Richard B. Buxton, Robert R. Edelman, Bruce R. Rosen, Gary L. Wismer, and Thomas J. Brady

Abstract: Partial saturation (PS) is an imaging technique that is useful in applications that require rapid image acquisitions (imaging time <1 min). Image contrast in PS imaging, as in other magnetic resonance methods, depends on the often conflicting effects of differences in proton density, T1, and T2. Previous analyses of pulse sequence optimization to maximize image contrast have assumed 90° pulses and examined the effects of varying repetition times (TR) and echo times (TE). In this paper we present theoretical calculations and images made with a 0.6 T imager to show that the radiofrequency pulse tip angle α, and not the pulse sequence timing parameters, is the most important parameter for producing image contrast. For large tip angles ($\alpha \geq 60°$), contrast is primarily determined by differences in T1, but for small tip angles ($\alpha \simeq 25°$), contrast is primarily due to differences in T2. The T2-weighted images can be produced as quickly as T1-weighted images by using a small pulse angle and a long TE; it is not necessary to use a long TR to reduce the effects of T1 differences. Optimum pulse angles are calculated, and the potential advantages and disadvantages of T2-weighted and T1-weighted PS imaging are discussed. **Index Terms:** Magnetic resonance imaging, techniques—Magnetic resonance imaging, physics—Magnetic resonance imaging.

Rapid magnetic resonance (MR) imaging, with an imaging time <1 min, is potentially useful in several applications: abdominal imaging, where respiratory motion artifacts can be significantly reduced by breath-holding (1,18); flow imaging (2–4); and dynamic studies following injection of contrast agents (5). With conventional imagers, rapid imaging can be done with either a partial saturation (PS) (4) or a conventional spin-echo (SE) pulse sequence. An advantage of PS imaging is that the patient receives fewer radiofrequency pulses; several image planes can be acquired in 20 s or less without excessive power deposition in the subject. To choose a pulse sequence for a particular application, the requirements for short imaging time and multislice capability must be balanced against image quality. A useful measure of the image quality is the contrast between two tissues with small differences in their relaxation times and spin density. For most tissues, differences in these basic MR parameters tend to be positively correlated; an increase in T1 is often accompanied by an increase in T2 and proton density. Because these differences have conflicting effects on the image contrast, pulse sequences are usually designed to emphasize differences in one parameter and to minimize the effects of the other parameters. To produce T1-weighted contrast, the repetition time (TR) is made short, magnifying the effects of longitudinal relaxation, and the echo time (TE) is made as short as possible to reduce the effects of transverse relaxation. Because the minimum imaging time is proportional to TR, T1-weighted images can be made quickly. To produce T2-weighted images, however, the effects of T1 differences are usually minimized by making $TR \gg T1$, and $TE \simeq T2$. Such images are often diagnostically useful, but the long imaging time used makes these images more susceptible to motion artifacts and precludes their use in any application requiring rapid images.

Many investigators have analyzed the effectiveness of different pulse sequences for producing

From the Department of Radiology, Massachusetts General Hospital and Harvard Medical School, Boston, MA. Address correspondence and reprint requests to Dr. R. B. Buxton at Division of Radiological Science and Technology, Massachusetts General Hospital, Fruit Street, Boston, MA 02114, U.S.A.

tissue contrast (6–12). These authors considered standard pulse sequences with fixed pulse angles of 90 or 180° and calculated optimum timing parameters. Although Ernst and Anderson (13) pointed out many years ago that a 90° pulse is not optimum for maximizing signal to noise, the effects of varying the pulse angle on image contrast are only beginning to be explored (14,15). In this article we show that the pulse angle, rather than the pulse timing parameters, is the single most important parameter for producing contrast in PS imaging. The pulse angle controls the character of PS image contrast; the relative importance of differences in T1 and T2 can be substantially changed by changing the pulse angle. With the appropriate pulse angle, T2-weighted images can be made as rapidly as T1-weighted images. Equations for the optimum pulse angles for maximizing sensitivity to differences in T1, T2, and proton density were calculated, and the contrast that can be achieved in a rapid T2-weighted image was compared with that of a rapid T1-weighted image. Finally, the relative importance of optimizing the pulse sequence timing parameters was examined.

THEORY

Signal Intensity in Partial Saturation Imaging

In PS imaging, slice selection in z and phase-encoding in y are done exactly as in standard SE imaging, but no 180° rephasing pulse is used (2). Instead, a gradient echo (or field echo) is produced in the course of frequency encoding the x-direction, by applying an x-gradient with opposite sign prior to the read gradient. The pulse sequence is simply a series of α-degree pulses with TR. A uniform group of spins subjected to this series of pulses will eventually reach a steady-state in which the magnetization returns to the same state before each pulse. If the pulse produces a rotation around the x-axis, the y-component of the magnetization immediately following a pulse in steady-state is (13):

$$My = \frac{M0 \sin(\alpha)\,(1 - E1)\,[1 - E2\cos(\theta)]}{[1 - E1\cos(\alpha)][1 - E2\cos(\theta)] - [E1 - \cos(\alpha)][E2 - \cos(\theta)]E2} \quad (1)$$

where E1 is exp(−TR/T1); E2 is exp(−TR/T2); α is the pulse angle; θ is the angle of precession from the y-axis in the x–y plane between pulses. The angle θ accounts for any precession of the spins between pulses. This can arise from off-resonance effects due to magnetic field inhomogeneities, susceptibility variations, or chemical shifts or from any field gradients applied between the pulses.

In an imaging experiment the signal is not measured immediately after the pulse because time is required to apply the imaging gradients. If the center of data acquisition is at TE after the pulse, the image intensity will be reduced by two effects due to the local line shape within a voxel. The first is the irreversible loss due to T2 decay, which we take to be a single exponential, exp(−TE/T2). The second effect is a loss in signal H(TE) due to the distribution of resonant frequencies within a voxel, produced by field inhomogeneity, susceptibility variations, or chemical shifts. In an SE pulse sequence the effect of H(TE) is reversed by applying a 180° refocusing pulse, but with a PS pulse sequence the effects of H(TE) will appear in the images.

The signal measured from a voxel in a PS image is a sum of the individual signals from the spin groups that make up the voxel. Because of the applied imaging gradients, the precession angle θ will have a range of values within the voxel. Defining $g(\theta)d\theta$ as the fraction of spins with precession angle between θ and $\theta + d\theta$, the image intensity of a voxel is

$$S = \int_0^{2\pi} \frac{d\theta g(\theta)\ S0 \sin(\alpha)\,(1 - E1)\exp(-TE/T2)\ H(TE)}{[1 - E1\cos(\alpha)] - W(\theta)} \quad (2)$$

where

$$W(\theta) = \frac{E2\,[E1 - \cos(\alpha)]\,[E2 - \cos(\theta)]}{[1 - E2\cos(\theta)]} \quad (3)$$

S0 is the image intensity that would be measured if $My = M0$. Equation 1 has been rearranged in forming Eq. 2 to combine all the terms involving E2 and θ into the term W. We assume in Eq. 2 that the x–y magnetizations of the spin groups within a voxel are distributed symmetrically around y so that only the y-components contribute in the integral.

The difficulty in analyzing PS imaging is in dealing with the precession angle θ. For an ideal system with no precession between pulses, $g(\theta) = \delta(\theta)$ and:

$$S = \frac{S0 \sin(\alpha)\,(1 - E1)}{[1 - E1\cos(\alpha)] + E2[E1 - \cos(\alpha)]} \quad (4)$$

Although this expression has been used to analyze PS imaging (14,15), it explicitly ignores the effects of the applied gradients used for imaging. If the effects are exaggerated by applying a spoiler gradient after data collection but before the next pulse, a reasonably well-defined state of magnetization will be produced in which all precession angles are equally likely within a voxel: $g(\theta) = 1/(2\pi)$. There is then no net x–y magnetization within a voxel before each pulse, although the spin groups that make up the voxel still retain some x–y magnetization unless $E2 \ll 1$. The resulting signal is

$$S = \int_0^{2\pi} \frac{d\theta\ S0 \sin(\alpha)\ (1 - E1)\ \exp(-TE/T2)\ H(TE)}{2\pi[1 - E1\cos(\alpha)] - W(\theta)} \quad (5)$$

This expression can be approximated when TR ≥ T2 (E2 ≪ 1) as:

$$S = \frac{S0 \sin(\alpha)\ (1 - E1)\ \exp(-TE/T2)\ H(TE)}{[1 - E1\cos(\alpha)]} \quad (6)$$

The accuracy of Eq. 6 was checked by numerically integrating Eq. 5 for a range of values of α, E1, and E2 with T1 = 10 T2. For TR = T2, the deviations of Eq. 6 from the full expression are at most ~10% for pulse angles between 10 and 90°. Equation 4, however, is significantly different from Eq. 5; for TR = T2 the errors are as high as 35% for the same range of pulse angles. Equation 6 is thus a better approximation than Eq. 4 for the signal intensity in an imaging experiment with imaging and spoiler gradients included and is valid as long as TR ≥ T2.

Effects of Line Shape

The image quality of PS images will degrade more quickly than SE images as TE increases, because phase changes produced by magnetic field inhomogeneities, magnetic susceptibility variations, and chemical shifts will not be refocused during data collection. For tissues containing both fat and water the chemical shift of the fat line will cause a periodic change in the signal intensity as TE is changed, because the two lines come in and out of phase (16). Although the enhanced effects of chemical shifts and magnetic susceptibility may be diagnostically useful (2,17), field inhomogeneities will simply decrease the signal. The function H(TE) that describes this signal loss is the Fourier transform of the distribution of resonance frequencies within a voxel. The magnitude of this effect can be estimated by assuming that the field varies linearly across a voxel with a range ΔB. Then H(TE) is

$$H(TE) = \frac{\sin(\lambda \Delta B\ TE)}{\lambda \Delta B\ TE} \quad (7)$$

where λ is the proton gyromagnetic ratio. For ΔB = 0.5 ppm at 0.6 T and TE = 60 ms, H(TE) = 0.9. So, for reasonable values of TE the dominant cause of signal decrease with increasing TE should be T2 decay. In the following analysis we have made the simplifying assumption that the effects of inhomogeneities are negligible for the TEs considered, and also that the tissues of interest do not contain appreciable fat, so that the chemical shift effects are also negligible.

Image Contrast

With the assumptions discussed above, the image intensity S in a PS image is

$$S = \frac{S0 \sin(\alpha)\ (1 - E1)\ \exp(-TE/T2)}{[1 - E1\ \cos(\alpha)]} \quad (8)$$

The contrast between two tissues in an image depends on the relative values of S0, T1, and T2 of the tissues. Differences in S0 will affect contrast in any pulse sequence, but the importance of differences in T1 or T2 can be controlled by adjusting the pulse sequence parameters α, TR, and TE. To produce a T1-weighted image the dependence of S on T2 is reduced by making TE as small as possible. To produce T2-weighted images the dependence of S on T2 must be increased by making TE ≈ T2, and the dependence on T1 must be reduced. This can be done in two ways: either TR can be increased, so that E1 → 0, as is done in conventional SE imaging, or α can be chosen to be very small so that cos(α) ≈ 1. In either case, S ≈ S0 exp(−TE/T2) sin(α), and thus image contrast will depend mainly on differences in S0 and T2.

A useful way to characterize the image contrast is to look at the sensitivity to small differences in the tissue MR parameters. The contrast (C) between a tissue of interest with proton density S0 and relaxation times T1 and T2 and another tissue with density S0 + ΔS0 and relaxation times T1 + ΔT1 and T2 + ΔT2 is approximately

$$C = \frac{\partial S}{\partial S0}\Delta S0 + \frac{\partial S}{\partial T1}\Delta T1 + \frac{\partial S}{\partial T2}\Delta T2 \quad (9)$$

In this article we are comparing relative contrast values for different pulse parameters, so it is not necessary to deal with the absolute magnitudes of the tissue differences ΔS0, ΔT1, and ΔT2. Rather, we define two parameters γ and β to describe the relative differences:

$$\gamma = \frac{\Delta S0/S0}{\Delta T1/T1} \quad (10)$$

$$\beta = \frac{\Delta T2/T2}{\Delta T1/T1} \quad (11)$$

Combining Eqs. 8–11 the contrast can be written as:

$$C = S0 \exp(-TE/T2)\frac{\Delta T1}{T1} \times \left[\frac{-TR}{T1}\frac{\sin(\alpha)\ [1 - \cos(\alpha)]\ E1}{[1 - E1\cos(\alpha)]^2} + \left[\gamma + \beta\frac{TE}{T2}\right]\frac{\sin(\alpha)\ [1 - E1]}{[1 - E1\cos(\alpha)]}\right] \quad (12)$$

From Eq. 12, the optimum pulse angle and TE for maximizing C can be calculated for any value of TR/T1. To examine the effect of varying TR, the appropriate quantity to compare is the contrast/noise ratio (C/N) that can be achieved in a fixed total imaging time (6–9,11,12). Because a shorter TR allows more signal averages in the same total time, and the noise level in an image depends just

on the number of averages, we can write C/N as (6):

$$\frac{C}{N} \propto \frac{C}{\sqrt{TR}} \qquad (13)$$

Note that for fixed TR, maximizing C from Eq. 12 is equivalent to maximizing C/N.

Equations 8–13 provide the basis for an analysis of image contrast in rapid PS imaging. The three pulse sequence parameters that can be controlled to maximize contrast are α, TE, and TR. For a particular pair of tissues with relative differences described by the parameters γ and β, the pulse tip angle that maximizes image contrast can be calculated from Eq. 12. For two ideal cases, (a) pure T1 contrast ($\Delta T2 = 0$ and $\Delta S0 = 0$) and (b) pure density and/or T2 contrast ($\Delta T1 = 0$), this calculation can be done analytically by differentiating Eq. 12 with respect to α, setting the result equal to zero, and solving for α. The optimum tip angles are then given by:

$$\cos(\alpha) = \frac{1 - 2E1}{E1 - 2} \quad \text{:pure T1 contrast} \qquad (14)$$

$$\cos(\alpha) = E1 \quad \text{:pure T2 and density contrast} \qquad (15)$$

The pulse angle given by Eq. 15 maximizes image signal to noise (13) as well as T2- or density-weighted contrast but is significantly different from the angle that maximizes T1-weighted contrast, as shown in Fig. 1.

Combined Effects of Differences in T1, T2, and S0

The analytic expressions in Eqs. 14 and 15 apply only to the ideal cases of tissues that differ in only one of the basic MR parameters. Most tissues will differ in all three parameters, although the differences in density will generally be much smaller than the differences in the relaxation times. Because these differences are often positively correlated (12), tissue contrast will usually be less than for these ideal cases. In general, the optimum pulse sequence will involve a balance between maximizing the sensitivity to one tissue parameter and minimizing the sensitivity to the other; Eqs. 14 and 15 only show how to maximize the sensitivity.

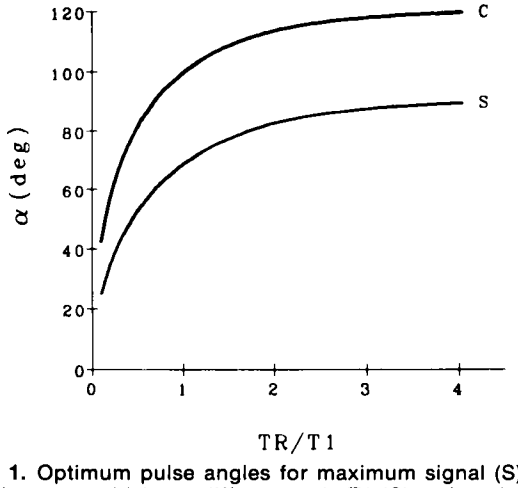

FIG. 1. Optimum pulse angles for maximum signal (S) and maximum sensitivity to differences in T1 (C) as functions of the repetition time (TR) for a partial saturation imaging sequence.

As an example of a more realistic pair of tissues, we have considered two tissues with equal fractional differences in T1 and T2 ($\beta = 1$) and compared the contrast that can be produced with a rapid T1-weighted sequence with that of a rapid T2-weighted sequence with the same TR. The sensitivity of the contrast to small changes in proton density was tested by considering the case of $\gamma = 0$ (no difference in density) and $\gamma = 0.2$. For T1-weighted images the effects of T2 differences can never be completely eliminated, because TE cannot be reduced to zero. We have assumed for these calculations that the minimum TE is TE = 0.2 T2, and used this value for calculating contrast for the T1-weighted images. For the T2-weighted image contrast calculations, we used TE = T2. Although this is not precisely the optimum TE, as will be shown below, it gives comparable image contrast.

Figures 2 and 3 show contrast as a function of pulse angle for the T1- and T2-weighted sequences calculated from Eq. 12 with TR = 0.2 T1. These curves show that the nature of the image contrast depends strongly on the pulse angle; small tip angles ($\alpha = 25°$) favor T2 contrast, and large tip angles favor T1 contrast. Furthermore, when there is no concurrent density difference, the T2-weighted contrast is somewhat lower than the T1-weighted contrast; but, with a positively correlated density difference, the T1 contrast is severely reduced (by 33%) whereas the T2-weighted contrast is boosted (by 28%). For this pair of tissues, the difference in density, although much smaller than the difference in the relaxation times, strongly affects whether T1- or T2-weighting will give better contrast.

The sensitivity of the contrast to the TE value used is shown in Figs. 4 and 5. The curves were calculated from Eq. 12 with a small tip angle ($\alpha = 25°$), appropriate for T2-weighted contrast and a larger tip angle ($\alpha = 70°$) appropriate for T1-weighted contrast. As in conventional imaging (7), the T1-weighted contrast is very sensitive to the minimum TE that can be used. If TE = 0.3 T2 is used instead of TE = 0.2 T2, the contrast will decrease by 24% for the case of no density difference ($\gamma = 0$) and by 31% if there is also a density difference ($\gamma = 0.2$). The T2-weighted contrast, however, is less sensitive; TE can be quite far from the optimum value and still produce reasonable image contrast, especially if there is also a positively correlated density difference.

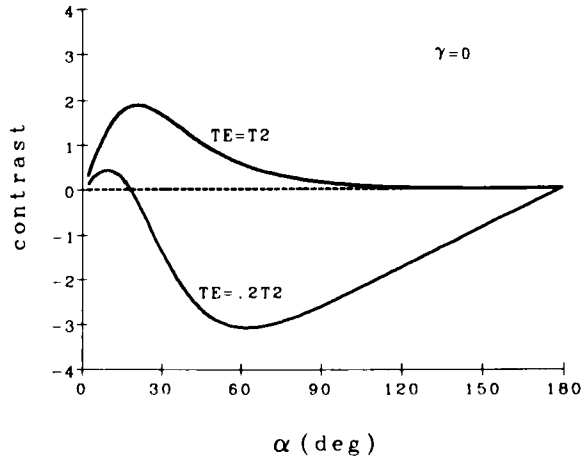

FIG. 2. Contrast (in arbitrary units) between two tissues with equal fractional differences in T1 and T2 ($\beta = 1$) and equal proton densities ($\gamma = 0$) as a function of the pulse tip angle. Curves were calculated with Eq. 12 for two values of the echo time: TE = 0.2 T2 (essentially T1-weighted contrast) and TE = T2 (essentially T2-weighted contrast).

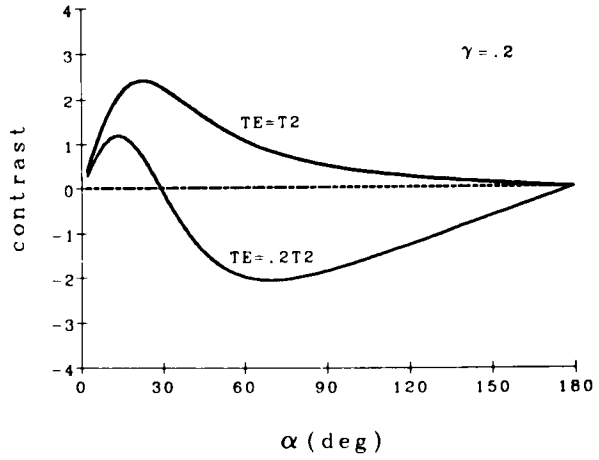

FIG. 3. Contrast calculated in the same way as for Fig. 2 but for two tissues with equal fractional differences in T1 and T2 ($\beta = 1$) and also with a positively correlated difference in proton density ($\gamma = 0.2$). For example, these curves would apply to tissues with a 10% difference in their relaxation times and a 2% difference in their proton densities.

Finally, the effect of varying TR on the C/N for equal total imaging time is shown in Figs. 6 and 7. For each value of TR/T1, the optimum pulse angles for T1- and T2-weighted contrast were calculated numerically from Eq. 12. The optimum pulse angle and the C/N calculated for that angle from Eq. 13 are both shown. For the T1-weighted sequences, the C/N improves as TR is shortened, and for the T2-weighted sequences the C/N is essentially independent of TR. For comparison, C/N for fixed 90° pulses in a PS image is also plotted. The key factor in producing high image contrast is thus not TR but rather the pulse angle α. With α optimized, the importance of TR is greatly reduced, especially for T2-weighted contrast.

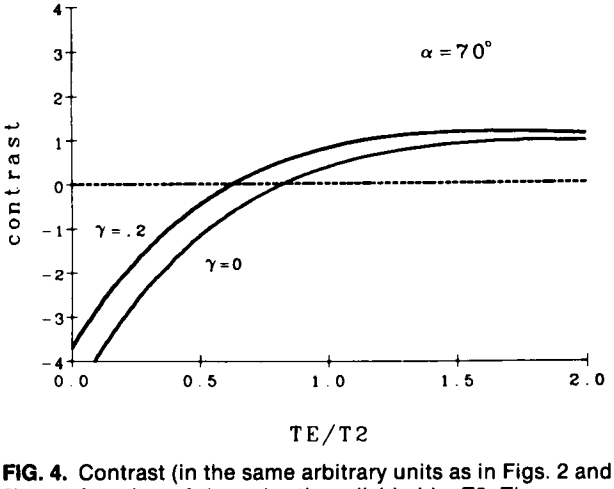

FIG. 4. Contrast (in the same arbitrary units as in Figs. 2 and 3) as a function of the echo time divided by T2. The curves were calculated from Eq. 12 with a pulse tip angle of $\alpha = 70°$ (T1-weighted) for two tissues with equal fractional differences in T1 and T2 and either equal proton densities ($\gamma = 0$) or a small positively correlated density difference ($\gamma = 0.2$).

MATERIALS AND METHODS

Imaging was done with a Technicare 0.6 T clinical whole-body imager to illustrate these theoretical results. To verify that signal decrease with increasing TE is primarily due to T2 decay and not to dephasing due to field inhomogeneities or susceptibility variations, we compared the decrease in signal of the liver, paraspinal muscle, and subcutaneous fat as TE was changed from 20 to 60 ms on PS images with the decrease on SE images. For liver the decrease on the two pairs of images differed by only 1%, muscle differed by 10%, and subcutaneous fat differed by 20%.

The larger difference for fat is probably due to chemical shift effects, and some fat may also be present in the region of interest over the muscle.

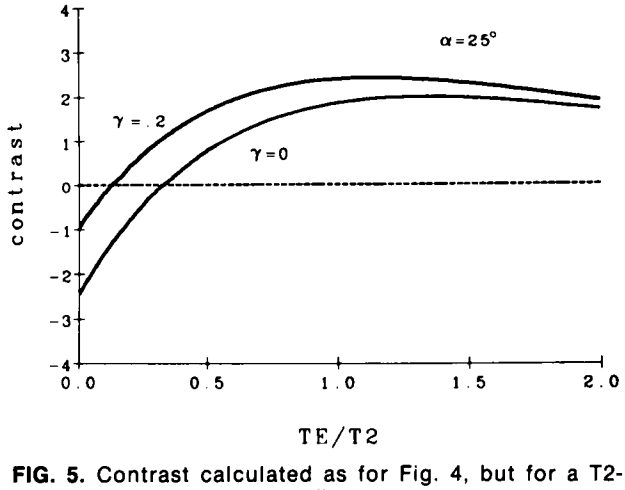

FIG. 5. Contrast calculated as for Fig. 4, but for a T2-weighted pulse angle ($\alpha = 25°$).

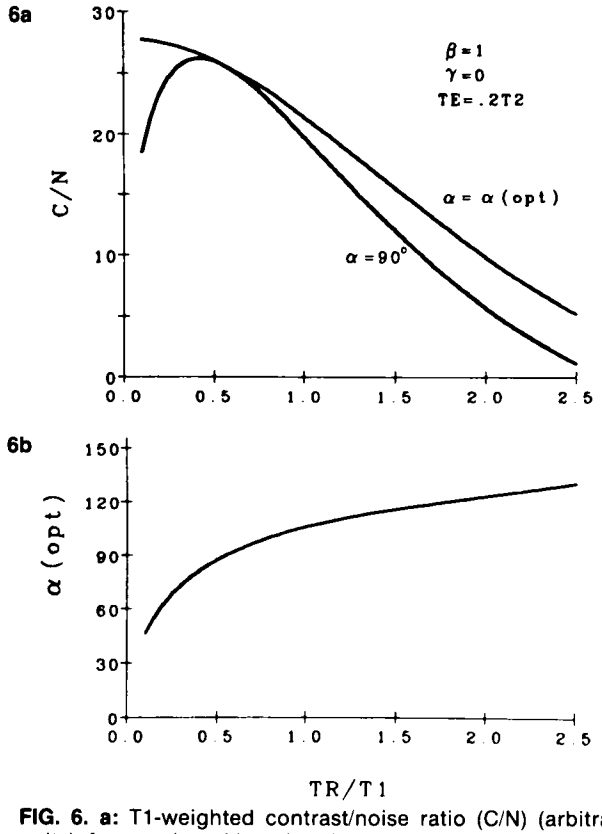

FIG. 6. **a:** T1-weighted contrast/noise ratio (C/N) (arbitrary units), for equal total imaging time, as a function of the repetition time divided by T1. The curves were calculated from Eqs. 12 and 13 for two tissues with equal fractional differences in their relaxation times (β = 1) and no difference in proton density (γ = 0), with TE = 0.2 T2. The upper curve shows the maximum C/N that can be achieved, by using the optimum pulse angle at each value of TR, and the bottom curve shows the C/N that results if the pulse angle is restricted to 90°, as in conventional imaging. **b:** The optimum pulse angle for the assumed tissue parameters used in the calculation of the upper curve in (a). The optimum was calculated numerically from Eq. 12.

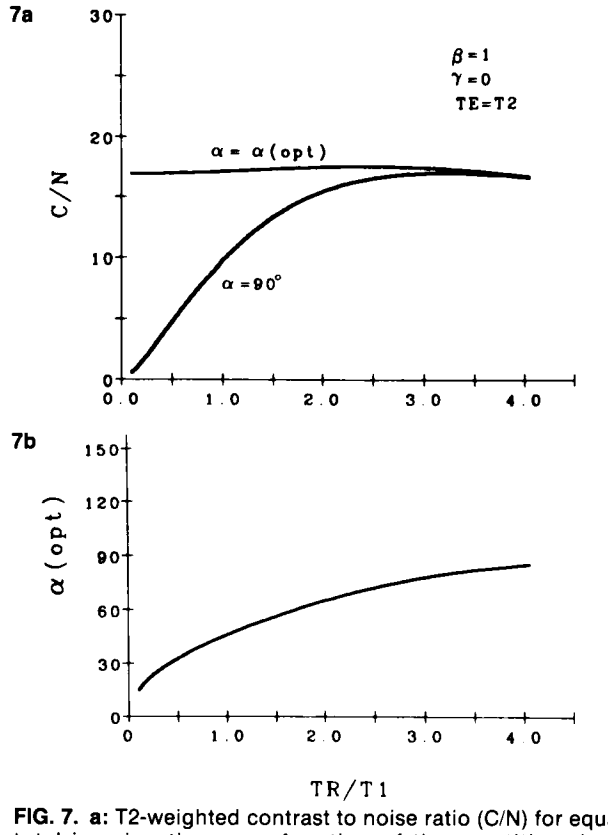

FIG. 7. **a:** T2-weighted contrast to noise ratio (C/N) for equal total imaging time as a function of the repetition time. Curves were calculated as for Fig. 6, except that TE = T2 to produce T2-weighting. **b:** Optimum pulse angle used in calculating the upper curve in (a).

For these tissues the errors in estimated T2 are comparable with the differences quoted above. Inhomogeneities thus are not a significant problem on our system, although chemical shift effects should be considered when examining tissues with fat. Abdominal images were then made of two normal subjects while breath-holding (20 s acquisitions), with TR = 100 ms for all images. Gaussian-shaped pulses were used, so the pulse angles do not correspond exactly to those calculated in the Theory section.

However, these images do show the qualitative features predicted by the theory. Figure 8 is a series of images made with TE = 11 ms and central pulse angles of ~75, 90, and 125°. Liver appears brighter than spleen, and the magnitude of the contrast varies with the pulse angle. Figure 9 is a series of T2/density-weighted images made with TE = 30 ms and central pulse angles of ~20, 30, and 50°. Liver/spleen contrast is reversed on these images, and the magnitude of the contrast depends strongly on the pulse angle. Region of interest measurements indicate that the contrast with a 20 or 50° pulse is only approximately half the contrast with a 30° pulse.

Figure 10 shows rapid T1 and T2/density-weighted images of the brain, with the expected reversal of gray matter/white matter contrast. For these images TR = 100 ms, TE = 16 and 50 ms, and the imaging time was 40 s.

DISCUSSION

The question of choosing the optimum pulse sequence parameters to produce the highest image contrast has received considerable attention in the MR literature (6–12). This study differs from previous studies in several ways, the most important of which is that we have considered the effects of varying the pulse angle. In this analysis we used an approximate expression for the signal intensity as a function of the pulse sequence parameters that is valid for TR ≥ T2, including the effects of gradients applied between the pulses. The gradients are assumed to produce a full range of precession angles within a voxel between pulses, so that there is no

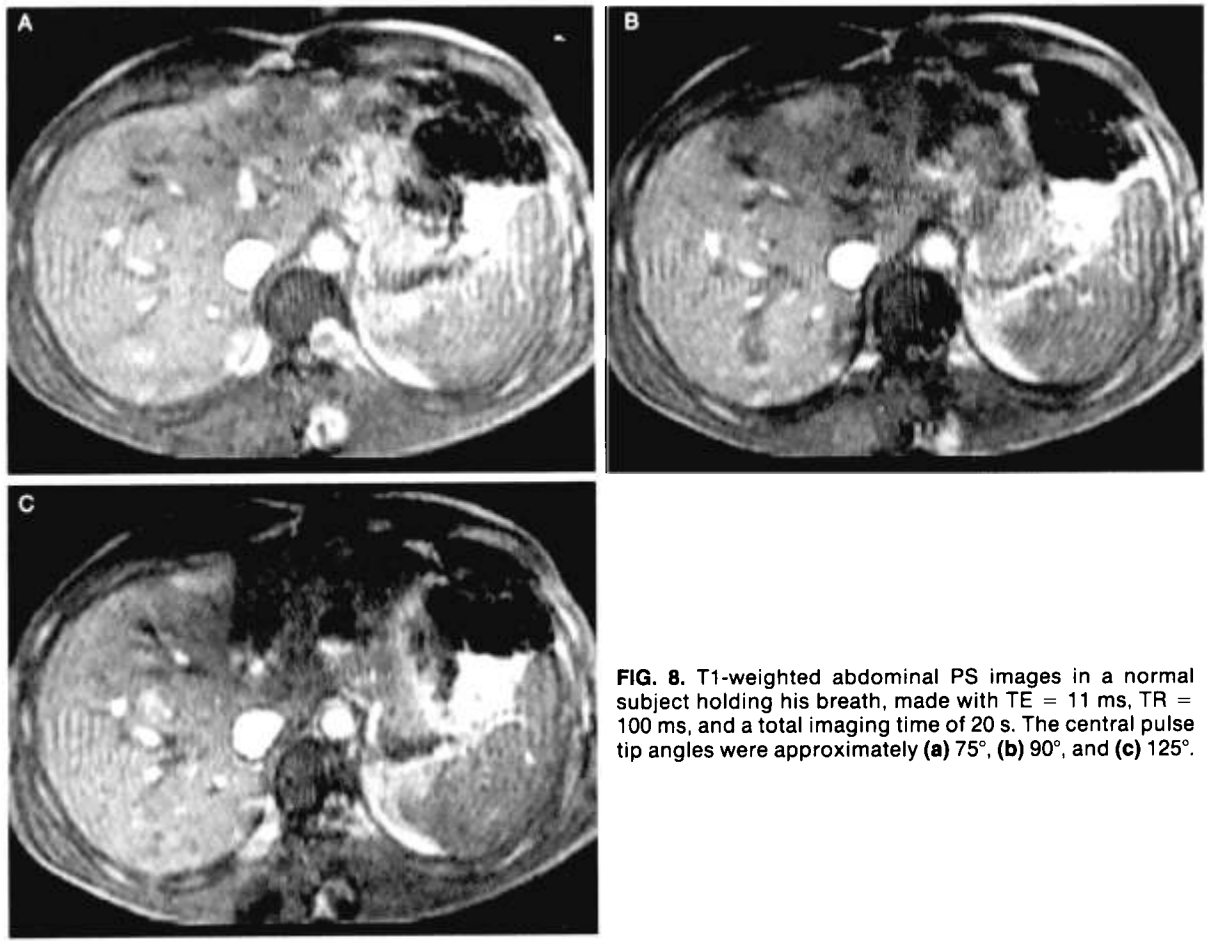

FIG. 8. T1-weighted abdominal PS images in a normal subject holding his breath, made with TE = 11 ms, TR = 100 ms, and a total imaging time of 20 s. The central pulse tip angles were approximately **(a)** 75°, **(b)** 90°, and **(c)** 125°.

net $x-y$ magnetization (although individual spin groups will retain some $x-y$ magnetization because T2 is comparable to TR). In a standard PS pulse sequence the gradient for slice selection is turned on before the next pulse, and the read gradient is left on for some time after data collection. Both of these gradients will produce a range of precession angles within a voxel, and, if necessary, their duration can easily be increased to ensure the conditions assumed above. For very short TR (TR $\ll$ T2) the character of the signal intensity changes as the steady-state effects become more pronounced, and the results shown here cannot be reliably extrapolated to this very rapid imaging regime.

The calculations show that for PS imaging the pulse angle is more important than the pulse timing parameters for producing tissue contrast. In this article we have treated contrast in the limit of small differences in the MR parameters. This differential approach is similar to the sensitivity calculations described by Mitchell et al. (8) and Moran (9). However, in this work we have specifically considered the conflicting effects of concurrent differences in T1, T2, and S0 and introduced the relative difference parameters γ and β to reduce the complexity of this more general problem. Hendrick et al. (7) and Wehrli et al. (11,12) analyzed C/N in standard imaging using the exact equations for contrast as the difference between two signals from tissues in which MR parameter differences are not necessarily small. Although more exact, the problem is not as easily analyzed with this approach, especially when the pulse angle is made a variable for optimization as well. Furthermore, the goal of pulse sequence optimization often is to be able to detect small deviations from normal; large deviations can be detected with many pulse sequences. The differential approximation used here should thus give reliable results.

Although analytic expressions for the optimum pulse angle can be found for certain ideal cases (Eqs. 14 and 15), the more general case of combined differences in the proton density and relaxation times is of greater interest. The theoretical calculations and the images shown demonstrate that the pulse angle is a crucial pulse sequence parameter for producing image contrast. As the pulse angle is increased, the character of the image contrast changes from being essentially T2-weighted to being T1-weighted. Echo time is also important, but in a more obvious way: TE must be reduced for T1-weighted contrast and increased to TE $\simeq$ T2 for

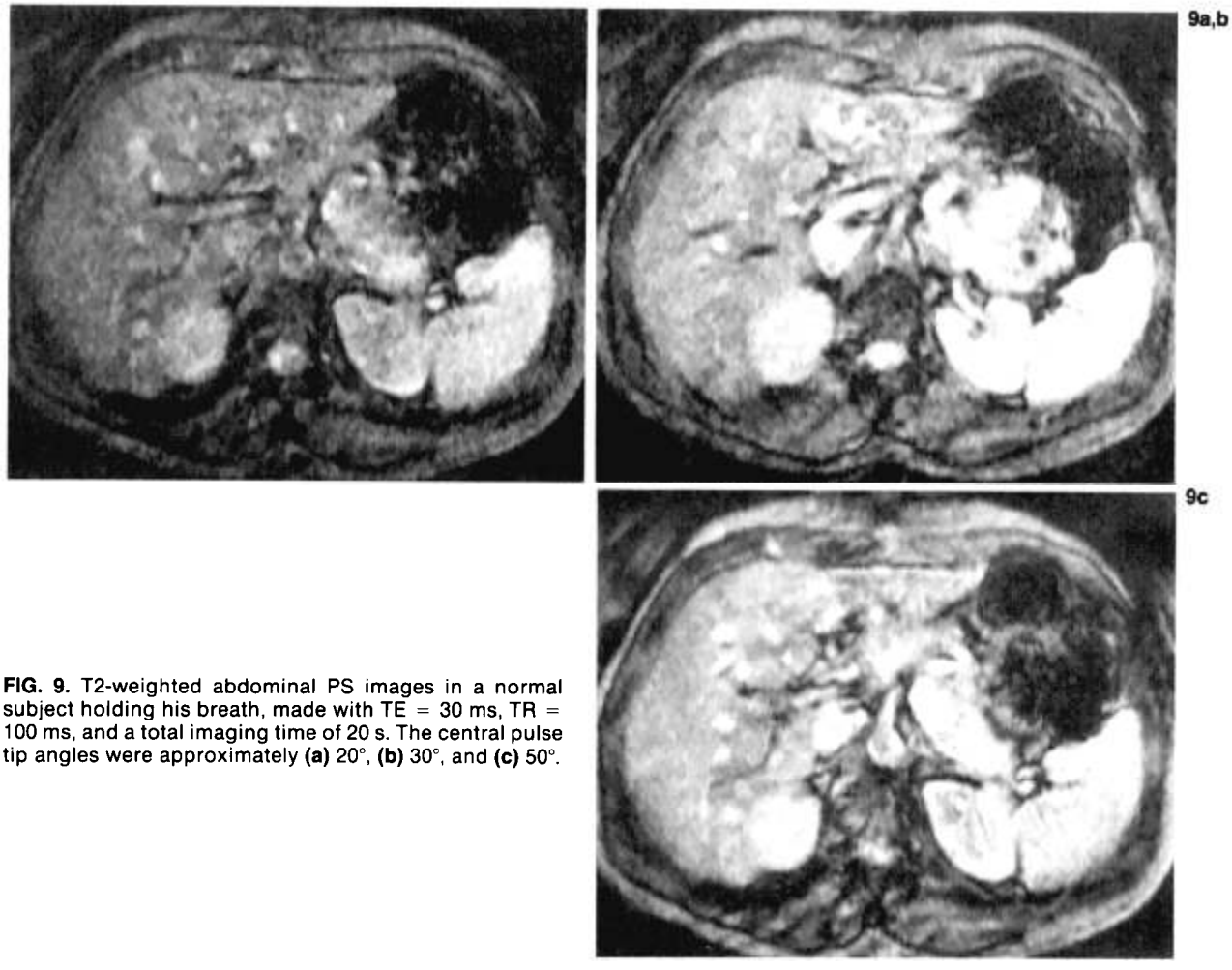

FIG. 9. T2-weighted abdominal PS images in a normal subject holding his breath, made with TE = 30 ms, TR = 100 ms, and a total imaging time of 20 s. The central pulse tip angles were approximately **(a)** 20°, **(b)** 30°, and **(c)** 50°.

T2-weighted contrast. For density-weighted contrast, both TE and the pulse angle must be reduced. However, TR is less important. For a fixed total imaging time the C/N in T2-weighted sequences is essentially independent of TR, and, although the C/N for T1-weighted sequences decreases with increasing TR, the curve is relatively flat for TR < T1. This is in sharp contrast to previous pulse sequence optimization calculations for standard PS and SE imaging with fixed 90° pulses, which show a sharp drop in C/N as TR is reduced below an optimum value. Once the pulse angle is optimized, the choice of TR becomes much less important; for rapid imaging it can be chosen to satisfy require-

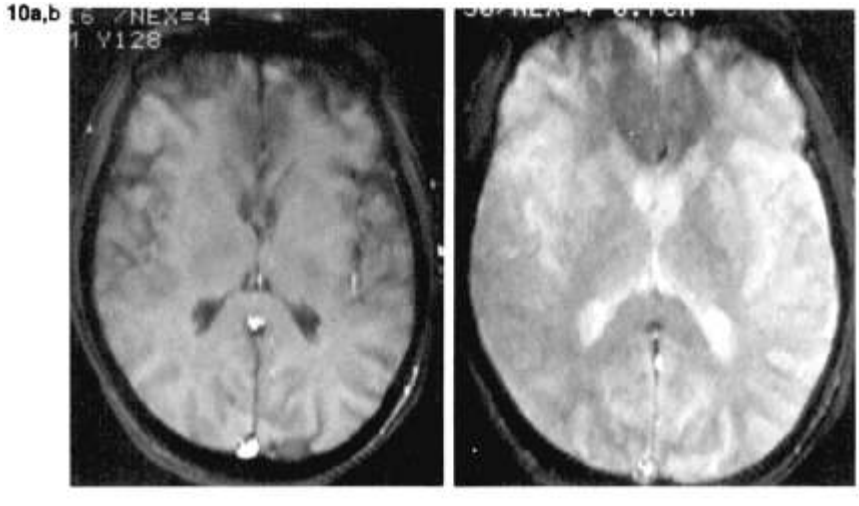

FIG. 10. Rapid PS images of the brain, made with TR = 100 ms and a total imaging time of 40 s. **a:** TE = 16 ms and the central pulse angle is ~120°. **b:** TE = 50 ms and the central pulse angle is ~30°.

ments for multislice imaging or imaging during breath-holding.

The T2-weighted images can be made as rapidly as T1-weighted images by choosing a small pulse angle and lengthening TE, and there are several factors that may favor T2-weighted imaging over T1-weighted imaging. Density differences associated with differences in the relaxation times are often such that contrast on a T1-weighted image is reduced and contrast on a T2-weighted image is increased (12). Such density differences are important for image contrast even when they are much smaller than the difference in T1. Another factor that may favor T2-weighted imaging is the image noise in one repetition of the pulse sequence. If the data collection time is reduced to produce a short TE for T1-weighted imaging (with larger imaging gradients to produce the same spatial resolution), the signal to noise will decrease. For T2-weighted imaging, TE is longer, so the data collection time can be as long as the intrinsic inhomogeneities of the magnet will allow. Finally, the effects of a slice-selective pulse may degrade the contrast in a T1-weighted image more than in a T2-weighted image. In these calculations we have assumed that each part of the image slice is tipped by the same pulse angle. This is certainly not true for Gaussian-shaped pulses, and even for more uniform sinc pulses there is some nonuniformity. For T2-weighted imaging with a small tip angle, this means that some parts of the slice will receive less than the optimum angle, but these smaller tip angles will still favor T2-weighted contrast. For the T1-weighted sequence, however, with a larger tip angle, some parts of the slice will be more T2-weighted, even with TE reduced. Selective pulses are thus likely to reduce T1 contrast more than T2 or density contrast.

The drawback to using T2-weighted PS pulse sequences is the enhanced effects of field inhomogeneities due to the longer TE. The seriousness of this problem will depend on the characteristics of each imager and the tissue being imaged. For tissues with a short T2, such as the liver, inhomogeneities will be less of a problem because the optimum TE is short. In our imager we see a negligible effect in the liver with TE = 60 ms. For tissues with a longer T2, it may be desirable to use TE values less than the theoretical optimum. However, as shown in Fig. 5, reasonable T2 contrast can be obtained with TE shortened substantially below the optimum.

A general treatment of image contrast in PS imaging is complicated by the increased sensitivity of the signal to variations in the local line shape as well as the spin density and relaxation times. In this analysis we have concentrated on the effects of variations in S0, T1, and T2, which are usually the primary source of image contrast. In some applications, however, effects due to chemical shift or susceptibility may be the dominant source of image contrast, and such images may be clinically useful (2,17). A general analysis of pulse sequence optimization including these effects has not yet been done.

CONCLUSION

For rapid MR ($T2 \leq TR \ll T1$) with a PS pulse sequence, the image contrast depends strongly on the chosen pulse angle. The T2-weighted images can be made as rapidly as T1-weighted images; the conflicting effects of T1 differences can be eliminated by making the pulse angle small. For T1-weighted images the optimum pulse angle is large and TE should be as short as possible, and for T2-weighted images the pulse angle should be much smaller with $TE \approx T2$. We have begun to use these pulse sequences routinely at our institution, and preliminary clinical results have been reported by Edelman et al. (17,18).

Acknowledgment: This work was supported in part by National Institutes of Health grant 1R01CA40303 and a grant from Technicare Corporation, Solon, OH, U.S.A.

REFERENCES

1. Haase A, Frahm J, Matthaei D, Hanicke W, Merboldt KD. Rapid NMR imaging using low flip-angles pulses. *J Magn Res* 1986;67:258–66.
2. Bydder GM, Young IR. Clinical use of the partial saturation and saturation recovery sequences in MR imaging. *J Comput Assist Tomogr* 1985;9:1020–32.
3. van Dijk P. Cardiac applications of flow imaging. Presented at the 4th annual meeting of the Society of Magnetic Resonance in Medicine, London, 1985. Berkeley, CA: SMRM.
4. Edelman RR, Wedeen V, Davis KR, et al. Multiphasic magnetic resonance imaging of pulsatile CSF flow. *Radiology* (in press).
5. Matthaei D, Frahm J, Haase A, Hanicke W. Regional physiological functions depicted by sequences of rapid magnetic resonance images [Letter]. *Lancet* 1985;2:893.
6. Edelstein WA, Bottomley PA, Hart HR, Smith LS. Signal, noise, and contrast in nuclear magnetic resonance (NMR) imaging. *J Comput Assist Tomogr* 1983;7:391–401.
7. Hendrick RE, Nelson TR, Hendee WR. Optimizing tissue contrast in magnetic resonance imaging. *Magn Reson Imag* 1984;2:193–204.
8. Mitchell MR, Conturo TE, Gruber TJ, Jones JP. AUR Memorial Award. Two computer models for selection of optimal magnetic resonance imaging (MRI) pulse sequence timing. *Invest Radiol* 1984;19:350–60.
9. Moran PR. A general approach to T1, T2, and spin-density discrimination sensitivities in NMR imaging sequences. *Magn Reson Imag* 1984;2:17–22.
10. Perman WH, Hilal SK, Simon HE, Maudsley AA. Contrast manipulation in NMR imaging. *Magn Reson Imag* 1984; 2:23–32.
11. Wehrli FW, MacFall JR, Glover GH, Grigsby N, Haughton V, Johansen J. The dependence of nuclear magnetic resonance (NMR) image contrast on intrinsic and pulse sequence timing parameters. *Magn Reson Imag* 1984;2:3–16.
12. Wehrli FW, MacFall JR, Shutts D, Breger R, Herfkens RJ.

Mechanisms of contrast in NMR imaging. *J Comput Assist Tomogr* 1984;8:369–80.

13. Ernst RR, Anderson WA. Application of Fourier transformation spectroscopy to magnetic resonance. *Rev Sci Instrum* 1966;37:93–102.
14. Young IR, Bryant DJ, Payne JA. Variations in slice shape and absorption as artifacts in the determination of tissue parameters in NMR imaging. *Magn Reson Med* 1985;2:355–89.
15. Young IR, Burl M, Bydder GM. Comparative efficiency of different pulse sequences in MR imaging. *J Comput Assist Tomogr* 1986;10:271–86.
16. Rosen BR. NMR proton chemical shift imaging [PhD Thesis]. Cambridge, MA: Massachusetts Institute of Technology, 1983.
17. Edelman RR, Johnson K, Buxton RB, et al. Magnetic resonance imaging of hemorrhage: a new approach. *AJNR* 1986;7:751–6.
18. Edelman RR, Buxton RB, Hahn PF, et al. Rapid magnetic resonance imaging with suspended respiration: initial clinical application in the abdomen. *Radiology* (in press).